Image Cover Sheet

CLASSIFICATION	SYSTEM NUMBER
UNCLASSIFIED	508793

TITLE

SECOND FLIGHT TEST OF A TOWBODY FOR A SQUID GRADIOMETER

System Number:

Patron Number:

Requester:

Notes:

DSIS Use only:

Deliver to:

National Defence
Research and Development Branch

Défense nationale
Bureau de recherche et développement

TECHNICAL MEMORANDUM 97/238
June 1997

SECOND FLIGHT TEST OF A TOWBODY FOR A **SQUID** GRADIOMETER

Harold S. Wilson — Richard J. Religa — Brian W. Dunstan

Defence Research Establishment Atlantic

Centre de Recherches pour la Défense Atlantique

Canada

DEFENCE RESEARCH ESTABLISHMENT ATLANTIC

9 GROVE STREET
P.O. BOX 1012
DARTMOUTH, N.S.
CANADA B2Y 3Z7

TELEPHONE: (902) 426-3100
FACSIMILE: (902) 426-9654

CENTRE DE RECHERCHES POUR LA DÉFENSE ATLANTIQUE

9 GROVE STREET
C.P. BOX 1012
DARTMOUTH, N.É.
CANADA B2Y 3Z7

National Defence
Research and Development Branch

Défense nationale
Bureau de recherche et développement

SECOND FLIGHT TEST OF A TOWBODY FOR A **SQUID** GRADIOMETER

Harold S. Wilson — Richard J. Religa — Brian W. Dunstan

June 1997

Approved by: R.E. Erickson
Head / Electromagnetics Section
Signature on File

TECHNICAL MEMORANDUM 97/238

Defence Research Establishment Atlantic

Centre de Recherches pour la Défense Atlantique

Canada

Abstract

This report presents the results of the second flight test of a towbody for a vertical-dewar superconducting magnetic gradiometer. The towbody was modified by the addition of a weight at the bottom in an attempt to reduce aerodynamic instabilities that were encountered in the first flight. Acceleration power spectra are presented and magnetometer slew rates and yaw, roll, and pitch amplitudes are given as tables. The pitching instability previously observed near 45 knots did not appear in this test and the high speed roll/yaw instability appeared only above 75 knots in level flight. The effect of magnetic contamination of the added weight is discussed and it is concluded that it should not be a problem during the flight test of a gradiometer. An Appendix gives the algebra required in the data analysis.

Résumé

Dans ce rapport nous présentons les résultats du second essai en vol d'un corps remorqué pour un gradiomètre magnétique supraconducteur ý vase de Dewar vertical. Le corps remorqué a été modifié par l'ajout d'un poids au fond dans l'effort de réduire les instabilités aérodynamiques éprouvées au cours du premier vol. Nous présentons les spectres de la force d'accélération et nous incluons, en forme de tables, les vitesses de balayage du magnétomètre ainsi que les amplitudes d'embardée, de roulis et de tangage. L'instabilité de tangage antérieurement observée près de 45 nœuds ne s'est pas manifestée au cours de cet essai et l'instabilité de roulis/embardée aux vitesses élevées s'est produite seulement au-dessus de 75 nœuds pendant du vol en palier. Nous discutons l'effet de la contamination magnétique du poids ajouté et nous concluons que ceci ne devrait poser aucun problème durant l'essai en vol d'un gradiomètre. L'algèbre nécessaire pour l'analyse des données se trouve dans un appendice.

Executive Summary

Report : DREA Technical Memorandum 97/238

Title : Second Flight Test of a Towbody for a SQUID Gradiometer

Authors : Harold Wilson, Richard Religa and Brian Dunstan

Security Rating : Unclassified

Background

The Surveillance and Ship Silencing Group at Esquimalt Defence Research Detachment (EDRD) of Defence Research Establishment Atlantic is investigating the feasibility of using SQUID magnetic gradiometers (SQUID = Superconducting Quantum Interference Device) to detect and localize targets in airborne antisubmarine warfare. This program involves investigations of the sources of noise in moving gradiometers, construction of a gradiometer under a contract with CTF Systems of Port Coquitlam, B.C., development of light-weight, low-power SQUID electronics and data-acquisition system, and construction of a towbody to allow a helicopter to carry the gradiometer. The object of the program is to demonstrate low gradiometer noise (~20 fT/m/$\sqrt{\text{Hz}}$) in a flight test.

EDRD's gradiometers are mounted in vertical dewars, so the towbody is essentially a vertical circular cylinder. Aerodynamically, it is a nonlifting body in a crossflow (i.e. at a 90° angle of attack), and there is very little in the technical literature on the flight characteristics of such bodies. Thus the results reported here will be of interest in other situations where a cylinder must fly at a very high angle of attack.

The first flight test of the towbody revealed two aerodynamic instabilities. The first would have increased system noise near 45 knots, but analysis of the data showed that it would be possible to use the towbody for a test of the SQUID gradiometer without modification. The second instability was more serious, and limited the towbody speed to 65 knots.

This report describes the second flight test in which a weight was added to the bottom of the towbody to lower the centre of gravity and to increase the pitch and roll moments of inertia. This has the effect of increasing aerodynamic stability.

Principal Results

The modification to the towbody eliminated the pitching instability near 45 knots and raised the onset of the high-speed roll/yaw instability to 75 knots. The aerodynamic origins of the instabilities are still not known.

Significance of the Results

The modified towbody is suitable for tests of the new superconducting gradiometer. There should be no increase in sensor noise due to increased pitching amplitudes near 45 knots.

Future Research

It would be useful to understand the origins of the aerodynamic instabilities revealed in the flight test. The aerodynamics of nonlifting bodies crossflows needs more attention.

Table of Contents

List of Tables

List of Figures

1. Introduction

The Surveillance and Ship Silencing Group at the Esquimalt Defence Research Detachment (EDRD) of Defence Research Establishment Atlantic is developing a new SQUID magnetic gradiometer (SQUID = Superconducting Quantum Interference Device) under a contract with CTF Systems, Inc., of Port Coquitlam, B.C. The gradiometer is scheduled to be tested in flight in late 1997 or in 1998. EDRD has built a towbody to carry the gradiometer, and this report describes the results of the second flight test of the towbody. The results of the first flight test of this towbody were presented in Ref.[1] and similar tests of a smaller towbody have been described previously in Refs.[2,3]. Since the towbody in this flight test was almost unchanged from the first test, and since the results presented here are similar to those in the earlier report, most of the details and background discussion are omitted. It is intended that this report will be accompanied by Ref.[1] which reported a mild pitching instability near 45 knots and a serious roll/yaw instability above ~70 knots.

Between the first and second flight tests, a weight was added to the bottom of the towbody, and the primary objective of the test described here was to see how this modification affected the aerodynamic instabilities of the towbody that Ref.[1] reported. The towbody was equipped with the same sensor package of a 3-axis magnetometer and 3-axis accelerometer that was used in the previous tests (Refs.[1-3]), and the data were analyzed by the same methods.

This report discusses briefly the towbody design and modifications since the first flight, and then the data analysis. Algebraic details are deferred to an Appendix. The flight characteristics are given in figures and tables in Section 5.

2. Towbody design and modifications

The towbody shown in Figure 1 is a vertical circular cylinder 1.97 m long and 0.44 m in diameter. We repeat the description in Ref.[1]. In flight it is suspended at its mid point by a long rope and the intention is to keep the cylinder upright. For this reason, the suspension point is at the centre, so there is only a small aerodynamic pitching moment. With its circular cross section, the towbody is a nonlifting body with a 90° angle of attack.

The top and bottom of the towbody are flat plates, a design which simplifies construction and reduces size, but this also increases drag and it may be responsible for eddy-shedding that leads to unstable flight. The only lifting surfaces which could exert a restoring pitching moment are the small flat plates which extend a short distance to the rear at the top and bottom.

The legs are designed to swing to the rear in flight. This provides some directional stability to the towbody and ensures that drag on the legs does not contribute to a forward pitching moment. The disadvantage of this scheme is that the legs and pivots move relative to the SQUID gradiometer, and if they are contaminated magnetically, the low-frequency magnetic noise will rise.

The principal modification to the towbody for the second flight was to replace the bottom plate with a fibreglass plate holding 18 kg of Pb shot set in epoxy as shown in Figure 2. The net effect is to

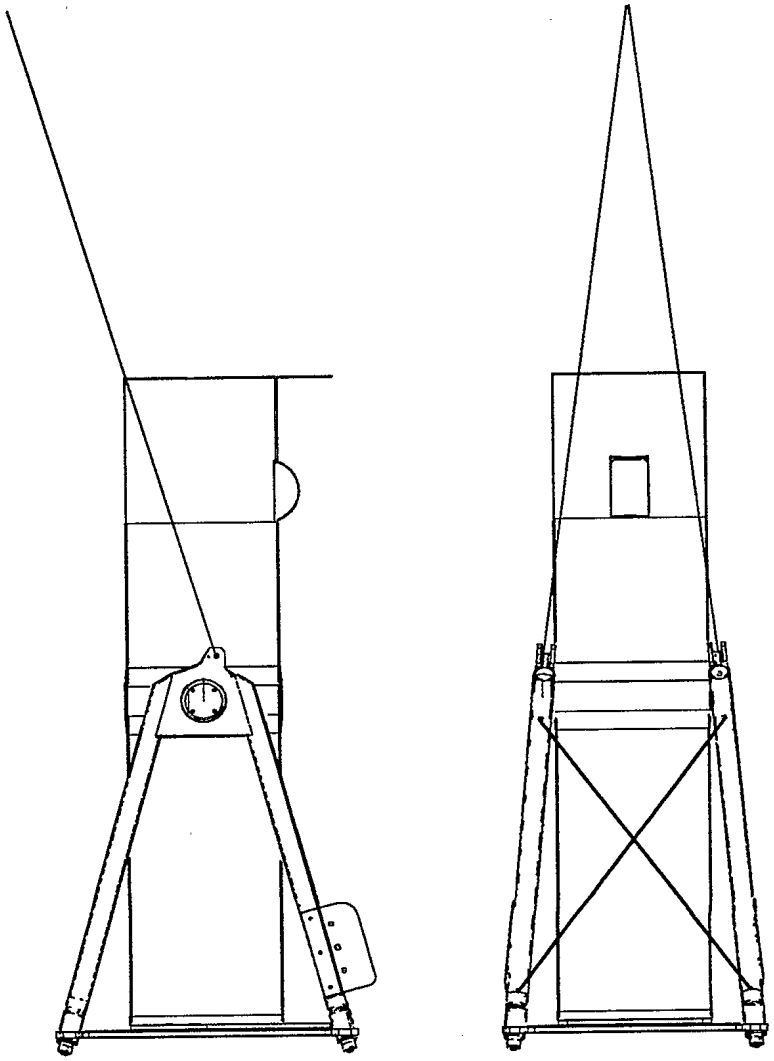

Figure 1 *The towbody and its connection to the tow rope. The fibreglass cylinder is 1.97 m long and 0.44 m in diameter. For the second flight, the weight of the bottom plate was increased by 17 kg. Left : left-side view. Right : rear view.*

increase the towbody mass from 147 to 164 kg and to lower the centre of gravity from 0.18 m below the pivot to 0.28 m below.

The design and elastic properties of the plate are important because fluctuating in-flight accelerations make magnetic contaminants in the plate move relative to the gradiometer, resulting in elevated noise. We present a simple estimate of the stiffness of the new bottom plate. Ref.[4], Table X, Case 1, gives a formula for the deflection of a circular plate supported at its edge under a load W distributed uniformly over the plate. The material parameters are E, the Young's Modulus, and m, the reciprocal of Poisson's ratio ; the plate parameters are the radius a and the thickness t. The average deflection is

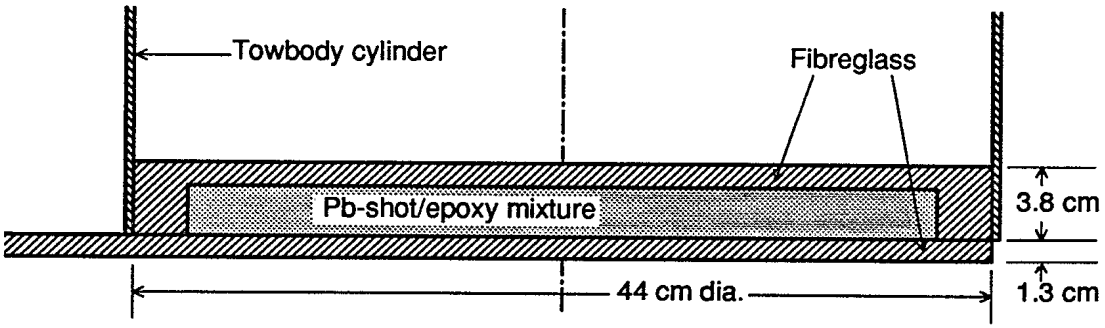

Figure 2 The new bottom plate of the towbody.

$$(\delta y)_{av} = \frac{Wa^2}{16\pi Et^3}\frac{(m-1)(7m+1)}{m^2} \quad , \tag{1}$$

and the average plate tilt is

$$|\delta\theta|_{av} = \frac{Wa}{5\pi Et^3}\frac{(m-1)(6m+1)}{m^2} \quad . \tag{2}$$

For fibreglass, we use $E=8\times10^5$ psi ($=5.5\times10^9$ N/m^2). Poisson's ratio for fibreglass is not known, so we assume that it lies in the range $0.16<\nu<0.5$ giving $2<m<6$. The biggest source of uncertainty is in the product Et^3 for the composite bottom plate shown in Figure 2. We assume that the Young's modulus of the Pb-shot, epoxy mixture is $E'=4\times10^5$ psi ($=2.8\times10^9$ N/m^2). Then the effective value of Et^3 is estimated as follows :

$$\left(Et^3\right)_{\text{eff}} = 12\int_{-t/2}^{t/2} E(\eta)\eta^2 d\eta \tag{3}$$

where η is the distance from the neutral surface of the plate, in this case the mid-plane (the neutral surface is neither compressed nor stretched during the deflection). Applying (3), the composite plate shown in Figure 2 has

$$(Et^3)_{\text{eff}} = 6.87\times10^5 \text{ N·m} \quad .$$

The plate will carry the weight of the gradiometer (90 kg) and the plate itself (20 kg). Then (1) and (2) show that the response to a 1-g acceleration will be an average deflection

$$(\delta y)_{av} = 6 \text{ μm } (m=2) \quad ,$$
$$9 \text{ μm } (m=6) \quad ,$$

and an average plate tilt

$$|\delta\theta|_{av} = 70\ \mu\text{rad}\ (m=2)\ ,$$
$$110\ \mu\text{rad}\ (m=6)\ .$$

The only other modification was to add 3-mm high strakes on the top 30 cm of the towbody where the fibreglass was particularly smooth in order to roughen the surface. This modification probably had no significant effect.

3. Flight details

The helicopter, tow-rope and data-acquisition systems were the same as in Ref.[1]. As before, the accelerometers were mounted 0.3 m above the suspension point.

The test consisted of straight, level flights of about 5 min duration at air speeds of 35, 44, 54 and 61 knots on intercardinal headings (i.e. near 45°, 135°, 225° and 315° magnetic neither horizontal magnetometer is aligned with magnetic north). Two runs were made at each speed on headings differing by 90°. A single run was done at 71 knots. The pilot had excellent control of speed and heading, with an RMS speed variation of <3 knots and an RMS heading variation of <3° on all runs.

In addition, the towbody stability was tested in climbs and descents of ±500 and ±1000 ft/min at speeds in the range 50-70 knots.

4. Data analysis

The data were analyzed in the same manner as in Ref.[1]. The yaw, roll and pitch amplitudes were determined by cross-power analysis and the acceleration spectra were determined from the Discrete Fourier Transforms of 216-s segments of data. The cross-power analysis is described below in the Appendix which corrects a sign error in the Appendix to Ref.[1], and extends the analysis to the situation in which the towbody exhibits a non-zero average roll angle.

Examination of the data showed that, as in the flight tests described in Refs.[1-3], the axes of the vector magnetometers and accelerometers were closely aligned with the transverse, forward and vertical axes of the towbody, where the transverse axis is defined by the suspension points of the towbody. The previous definition of towbody orientation angles was used here :

(i) Positive yaw (ϕ) $\Longrightarrow$ towbody turns to the right ,

(ii) Positive roll (ρ) $\Longrightarrow$ right side goes down ,

(iii) Positive pitch (ψ) $\Longrightarrow$ top moves forward .

The drag was not measured during the second flight. Since the external shape of the towbody was the same as in the first flight, the drag coefficient would be the same as reported in Ref.[1] :

$$C_D = 1.18 \pm 0.09.$$

5. Test results

5(i) Acceleration spectra

The accelerometers were mounted 0.3 m above the suspension point of the towbody (i.e. above the pitch axis). This means that for the well-defined pitch motion at 0.7 Hz, the accelerations recorded were significantly higher than the accelerations that will be felt by the gradiometer pickup loops which will be located 0.75 m below the axis (above the pitch axis, the linear acceleration due to the pitching has the same sign as the acceleration due to gravity ; below the axis, the signs are opposite).

Figure 3 shows the acceleration spectra measured at 35, 44, 54, 61 and 71 knots airspeed. In each case, the data were analyzed as a single 216-s segment (8192 points at the sample rate of 37.88/s). A cosine taper of 512 points was applied to each end of the data segment. The analog signals were filtered with an order-1 3.88-Hz low-pass filter at the input to the ADC. Except for 71-knot data, the spectra shown are the average of two runs. During the flights, the airspeed was recorded every 30 seconds and the notebook shows that the RMS variation in the speed was <3 knots.

The spectra in Figure 3 and visual examination of the time series show no sign of the pitching instability that was observed during the first test flight in the speed range 45-50 knots. The speed control was better in the second flight, so a pitching instability that occurred only in the 47-51 knot range might not appear in these data. However, such a narrow resonance seems unlikely.

Comparison of the vertical accelerations in Figure 3 and in Figure 2 of Ref.[1] shows that the 4-Hz signal was significantly larger in the second flight. We do not know the physical origin of this signal, so we cannot say anything about it except that it must originate in tension fluctuations in the tow rope since it does not appear in the other accelerometers.

Table I. 99th percentile slew rates for the transverse, forward and vertical magnetometers (T,L,V). The absolute slew rate was less than the tabulated value for 99% of the data. Compare to Table II of Ref.[1].

Speed (knots)	Heading (deg)	$\lvert dB_T/dt \rvert$ (nT/s)	$\lvert dB_L/dt \rvert$ (nT/s)	$\lvert dB_V/dt \rvert$ (nT/s)
35±3	132	2600	5000	1400
34±3	233	2200	5600	1200
44±3	145	3100	6600	1650
44±3	060	8400	7900	1450
53±2	322	10000	8400	2550
54±2	229	2800	7400	1900
60±2	139	3100	10300	3200
61±3	058	10000	10300	2900
71±2	230	5100	13000	3300

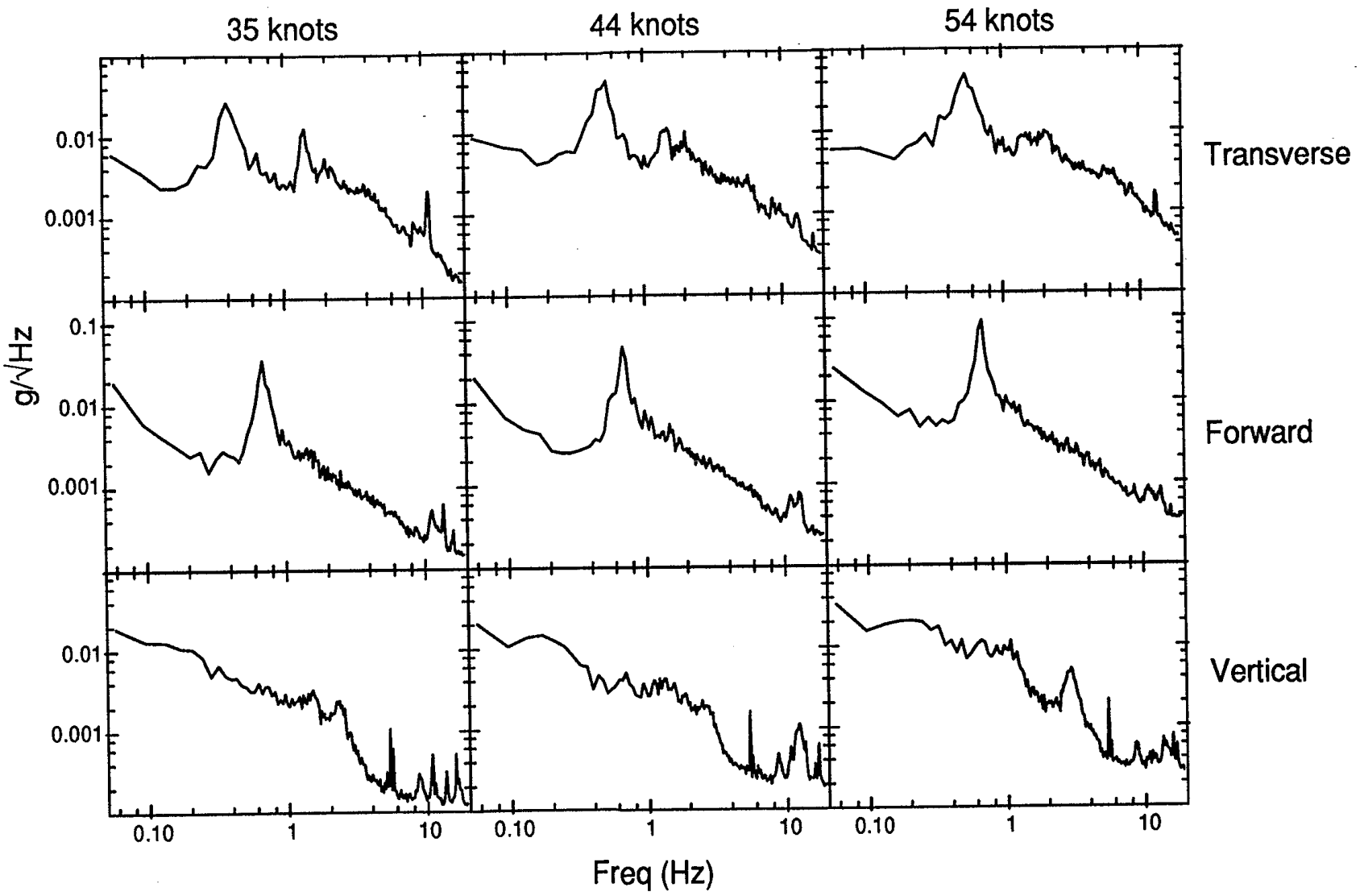
35 knots
44 knots
54 knots
Transverse
Forward
Vertical
g/√Hz
0.1
0.01
0.001
0.10
1
10
Freq (Hz)

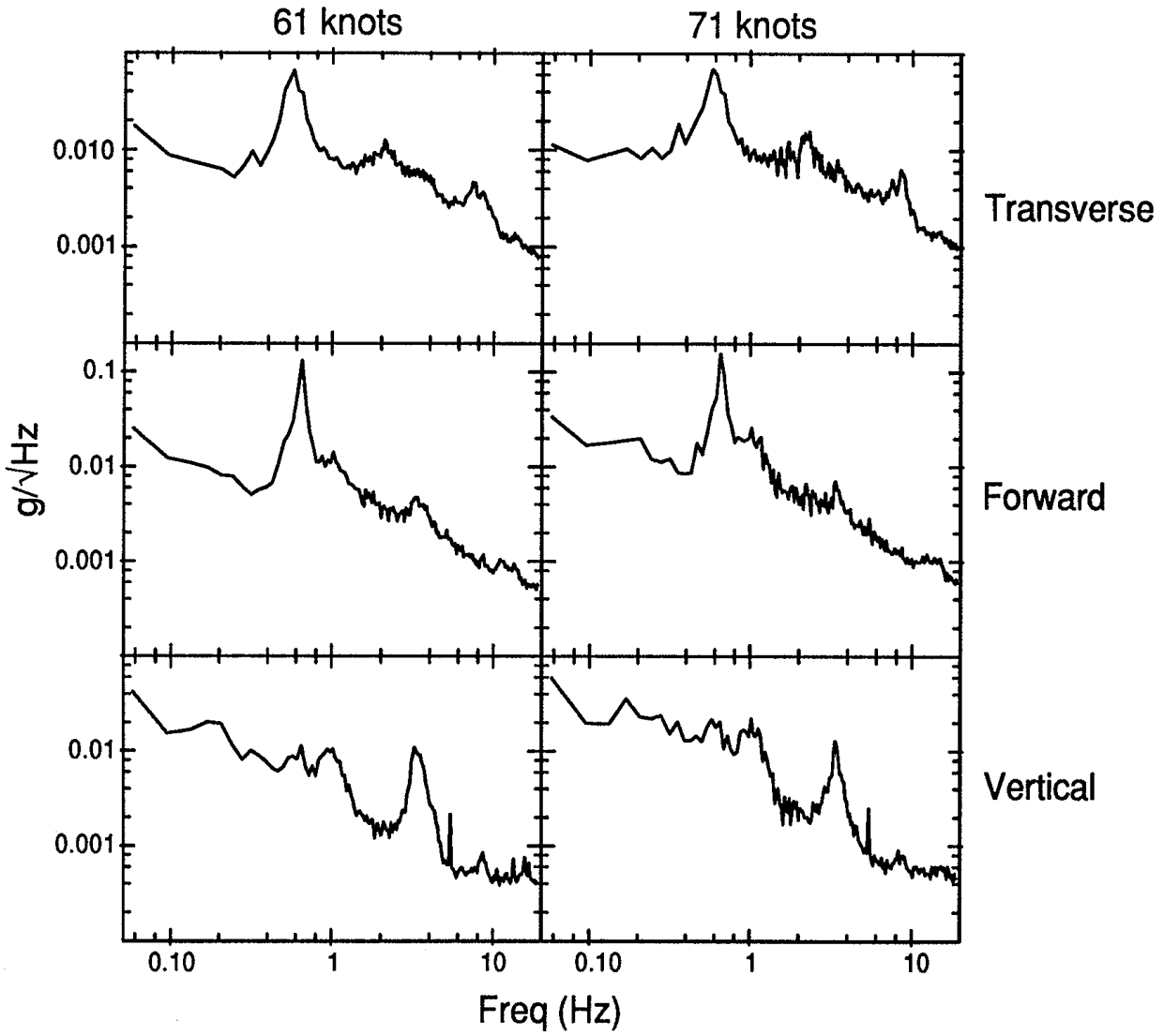

Figure 3 *Acceleration noise spectra for straight, level flight. The spectra are smoothed with $\delta f=0.037$ Hz for $f<1.85$ and $\delta f=0.02f$ for $f>1.85$ Hz. The spectra plotted are the average of two runs of 216 s, except for 71-knots which is calculated from one 216-s run.*

5(ii) Magnetometer slew rates

Ref.[1] discussed the significance of magnetometer slew rates as a source of electronic noise in mobile SQUID gradiometer systems and noted that we must have magnetometer slew rates <45000 nT/s. Table I lists the slew rates observed in straight, level flights on intercardinal headings. These values are often somewhat higher than the results reported in Table II of Ref.[1] and the difference is attributed mostly to the effect of towbody heading : the magnetometers are more sensitive to pitch and roll motions on some headings than on others.

5(iii) Roll and pitch motions

Between 0.1 and 2 Hz, the towbody motion is dominated by a 0.5-Hz roll and a 0.7-Hz pitch as shown in the accelerometer spectra in Figure 3. The yaw, roll and pitch amplitudes were determined by analysis of the cross-power spectra of the 3 magnetometer signals and the forward accelerometer as described in the Appendix. The results of the analysis are listed in Table II which may be compared to Tables III and IV of Ref.[1].

The pitching amplitudes are not significantly reduced from the first flight, except that the pitching instability near 45 knots that was seen earlier has disappeared. The pitch amplitude at 61 knots is actually a little higher than in the first flight. The severe instability observed above 70 knots in the first flight does not appear in the 71-knot data although the pitch amplitude reaches 1.3°(RMS) and the roll amplitude is 0.8°(RMS).

Table II The amplitudes of the roll/yaw and pitching motions of the towbody. These motions appear as peaks in the transverse and forward accelerometer spectra. Except for the 71-knot results, the tabulated amplitudes are from two runs averaged in quadrature. These results may be compared to Tables III and IV of Ref.[1].

	Roll/yaw motion				Pitch motion			
Speed (knots)	Freq. (Hz)	Yaw (° RMS)	Roll (° RMS)	Pitch (° RMS)	Freq. (Hz)	Yaw (° RMS)	Roll (° RMS)	Pitch (° RMS)
35	0.41	2.3	0.43	0.06	0.70	0.4	0.08	0.34
44	0.50	2.3	0.60	0.13	0.69	0.5	0.13	0.42
54	0.54	1.3	0.52	0.17	0.68	1.0	0.28	0.84
60	0.55	1.7	0.67	0.40	0.65	1.3	0.42	1.04
71	0.57	1.6	0.77	0.57	0.66	1.0	0.39	1.33

Table II shows that the towbody with the extra 17 kg of weight in the bottom plate is stable at airspeeds up to 70 knots.

5(iv) Static pitch and roll

Analysis of the average output of the transverse and forward accelerometers during the straight, level flights gave the average pitch and roll angles, which are listed in Table III. A surprising result of the analysis of this test was the appearance of a large static roll above 55 knots. The source of the roll is not known. At low speeds, the drag on the towbody is low so the tow rope is nearly vertical and the rope suspension provides roll stability. At higher speeds, the tow rope becomes more horizontal and the roll stability is determined by the weight of the towbody acting at the center of gravity. However, even at 70 knots with a drag coefficient C_D=1.2, the drag on a 164-kg towbody should result in a rope angle that is only 26° from vertical, and this should still hold the towbody level.

It is not known why the towbody pitch is slightly negative at 35 knots, but it may be related to interference between the bridle (see Figure 1) and the sides of the towbody when the tow rope is nearly vertical.

5(v) Roll/yaw instability at high-speed

The roll/yaw instability reported in Ref.[1] appeared in this flight test also, but only when the air speed exceeded 75 knots in level flight, and above 70 knots in a descent of 500 ft/min. The pitch and roll amplitudes shown in Table II show that even at 71 knots in level flight, the towbody was not rocking badly. The sudden appearance of a static roll above ~60 knots may be related to the onset of the roll/yaw instability at higher speeds.

Table III Static roll and pitch angles determined from the transverse and forward accelerometers.

Speed (knots)	Static roll ρ_0 (deg)	Static pitch ψ_0 (deg)
0 (on ground)	0.0	
0 (hovering)	-0.7	
35	0.3	-2.0
44	0.8	1.2
54	0.3	1.6
61	-3.4	1.8
71	-3.9	1.9

6. Magnetic noise due to bottom-plate contamination

The two fibreglass parts of the bottom plate and the Pb shot were scanned with an optically-pumped total-field magnetometer. Magnetic contamination of the fibreglass produces a magnetic field of ΔB~0.08 nT at a distance r=11 cm above the plate. The Pb shot is also slightly contaminated, but it produces a much lower field (~0.015 nT at 11 cm). Thus the magnetic moment of the contaminants is roughly

$$\left|\vec{M}\right| \sim \Delta B \cdot r^3 = 106 \text{ nT} \cdot \text{cm}^3 \quad . \tag{4}$$

This section estimates the magnetic noise due to motion of the contaminant moment $\vec{M}$ relative to the gradiometer. It is assumed that $\vec{M}$ is due to permanently-magnetized contaminants in the fibreglass and Pb shot.

6(i) Bottom-plate bending

The elastic deflection of the bottom plate was estimated in Section 2. The effect of a small rotation of the magnetic moment causes an "average gradient" change

$$(\delta G)_{AV} = \sqrt{\left\langle \delta G_{ij} \cdot \delta G_{ji} \right\rangle} \sim \frac{\sqrt{15}M}{R^4} \delta\theta \quad , \tag{5}$$

where the average is an RMS average over relative orientations of $\vec{M}$ and $\vec{R}$. A small change in the separation causes an "average gradient" change

$$(\delta G)_{AV} = \sqrt{\left\langle \delta G_{ij} \cdot \delta G_{ji} \right\rangle} \sim \frac{4\sqrt{30}M}{R^5} \delta R \quad . \tag{6}$$

In the new SQUID gradiometer, the pickup loops will be located only 26 cm above the bottom plate. Section 2 estimated that a 1-g acceleration will cause an average plate deflection of ~8 μm and an average tilt of ~100 μrad, while Figure 3 shows that a vertical acceleration of 0.04 g/√Hz overestimates the vertical accelerations. Thus the spectrum of distance and tilt fluctuations is approximately δR~0.3 μm/√Hz and $\delta\theta$~4 μrad/√Hz. Substituting for M, R, δR and $\delta\theta$ in (5) and (6) gives

$$(\delta G)_{AV} = 6\times10^{-7} \text{ nT/m/}\sqrt{\text{Hz}} \text{ due to deflection}$$

and

$$(\delta G)_{AV} = 4\times10^{-7} \text{ nT/m/}\sqrt{\text{Hz}} \text{ due to tilting} \quad .$$

The noise level specified for the new gradiometer is 1×10^{-5} nT/m/√Hz from each of several sources, so these estimates indicate that noise due to elastic bending of the contaminated bottom plate should not be a problem.

6(ii) Compression of the SQUID gradiometer.

The SQUID gradiometer is carried by the outer wall of its liquid-helium dewar. When the dewar is accelerated, the walls are compressed and the gradiometer pickup loops move closer to the bottom of the dewar and the magnetically-contaminated bottom plate, resulting in magnetic noise. (SQUID-gradiometer design is discussed in Refs.[5,6].) This section makes an estimate of the dewar-wall compression in response to a vertical acceleration.

The new gradiometer that is being built for DREA by CTF Systems has a fibreglass dewar with outer diameter 0.44 m, wall thickness 5.1 mm and length 1.46 m. The total weight carried by the outer dewar wall may be as high as 90 kg. As noted Section 2, Young's modulus for fibreglass is $\sim 5.5\times10^{9}$ N/m^2. With an acceleration of 0.04 g/$\sqrt{\text{Hz}}$, the vertical motion of the top plate of the dewar (and hence the gradiometer that is suspended from it) is

$$\delta R = 1.5\ \mu\text{m}/\sqrt{\text{Hz}} \quad .$$

This seems ridiculously small for a 90 kg weight on a 1.6-m long, thin-walled structure, but it must be remembered that this is the response to load fluctuations of only 3.6 kg(force) $\sqrt{\text{Hz}}$. Substituting in (6) shows that this will result in gradient noise of

$$(\delta G)_{AV} = 3\times10^{-6}\ \text{nT/m}/\sqrt{\text{Hz}} \quad .$$

This is more severe that the magnetic noise due to bottom-plate deflection, but it is still much less than the noise specification of 1×10^{-5} nT/m/$\sqrt{\text{Hz}}$ specified in the contract for the new gradiometer.

7. Conclusions

The weight added to the bottom plate of the towbody eliminated the pitch instability near 45 knots that was reported by Ref.[1]. While the 45-knot pitch instability was not a critical problem for a flight test, it is reassuring to know that large-amplitude pitches will not appear in the 45-50 knot speed range. With the heavier base plate, the high-speed roll/yaw instability does not appear until the air speed exceeds 75 knots in level flight.

A static roll appeared above ~55 knots. It may be related to the appearance at high speeds of the severe roll/yaw instability. Since the towbody is symmetric, the appearance of a static roll is surprising and we have no explanation for it.

Magnetic contamination in the new base plate is not a major problem because the dewar and towbody are sufficiently stiff that there will be very little fluctuation in the gradient of the contaminant magnetic field. This conclusion assumes that the magnetic contamination is permanently-magnetized steel chips in the fibreglass and Pb-shot. EDRD's experience with magnetic contamination indicates that this is a fair assumption.

Acknowledgements

Mr. J.B. Nelson of EDRD and Dr. P. Kubik of CTF Systems reviewed drafts of this report and made suggestions for improving the presentation.

References

[1] H. Wilson, B. Dunstan and R. Religa, "Flight Test of a Towbody for an Airborne Vertical SQUID Gradiometer", DREA Technical Memorandum 97/212 January 1997

[2] D. Hopkin and H. Wilson, "Design and Test of a Towbody for an Airborne SQUID Gradiometer", DREP Technical Memorandum 92-44 October 1992

[3] H. Wilson, et al., "Flight Test of a Cylindrical Towbody for an Airborne SQUID Gradiometer", DREP Technical Memorandum 94-16 March 1994

[4] R.J. Roark, Formulas for Stress and Strain, 3rd edition, McGraw-Hill 1954

[5] H. Wilson, "Limitations to SQUID Gradiometer Sensitivity", DREP Report 88-2 Sept. 1988

[6] K.Betts, et al., "Investigation and Design of a Superconducting Magnetic Gradiometer", DREP Contractor's Report 92-27 May 1992

Appendix

Data Analysis Algebra

This Appendix gives the straightforward algebra of rotation matrices and cross-power spectra which is used in the analysis of the magnetometer and accelerometer signals. It repeats the Appendix to Ref.[1], but with two typographical errors corrected, and with the algebra extended to the case of non-zero average roll.

(i) Coordinate systems

Two coordinate systems are used in the analysis :

1. Space fixed. Basis vectors : $\hat{u}_1 =$ magnetic east , $\hat{u}_2 =$ magnetic north , $\hat{u}_3 = \hat{u}_1 \times \hat{u}_2 =$ up ;
2. Body fixed. Basis vectors : $\hat{e}_1 =$ right , $\hat{e}_2 =$ forward , $\hat{e}_3 = \hat{e}_1 \times \hat{e}_2$.

(ii) Rotation Matrix

The towbody orientation is defined by three successive simple rotations that take the space-fixed into the body-fixed basis vectors :

1. Yaw by angle ϕ clockwise around $\hat{u}_3$ ($\phi>0 \Rightarrow$ turn to the right).
2. Roll by ρ counterclockwise around $\hat{e}_2(\phi,0,0)$ ($\rho>0 \Rightarrow$ right side goes down).
3. Pitch by ψ clockwise around $\hat{e}_1(\phi,\rho,0)$ ($\psi>0 \Rightarrow$ top goes forward).

The rotation matrix M is defined in terms of the effect of the rotation on a body-fixed vector : before the rotation, $\vec{R} = R_\nu \hat{u}_\nu$. The rotation (ϕ,ρ,ψ) takes it to $\vec{S} = R_\mu \hat{e}_\mu = S_\nu \hat{u}_\nu$. The rotation matrix is defined by

$$S_\mu = M_{\mu\nu} R_\nu \quad . \tag{A-1}$$

The complete expression for the rotation matrix is

$$M = \begin{bmatrix} \cos\phi\cos\rho & \sin\phi\cos\psi - \cos\phi\sin\rho\sin\psi & \sin\phi\sin\psi + \cos\phi\sin\rho\cos\psi \\ -\sin\phi\cos\rho & \cos\phi\cos\psi + \sin\phi\sin\rho\sin\psi & \cos\phi\sin\psi - \sin\phi\sin\rho\cos\psi \\ -\sin\rho & -\cos\rho\sin\psi & \cos\rho\cos\psi \end{bmatrix} . \tag{A-2}$$

(iii) Accelerometer signals

This section gives the output of a rotating linear accelerometer assuming no linear acceleration of the centre of rotation. The accelerometer gain vector is

$$\vec{a} = a_\mu \hat{e}_\mu \quad \text{(Body-fixed)},$$

the accelerometer position relative to the centre of rotation is

$$\vec{R} = R_\mu \hat{e}_\mu \quad \text{(Body-fixed)},$$

and the acceleration of gravity is

$$\vec{g} = g_\nu \hat{u}_\nu \quad \text{(Space-fixed; } g_1=g_2=0,\ g_3=9.8\ \text{m/s}^2\text{)} .$$

Then the accelerometer output due to rotations is

$$A(t) = \vec{a}(t)\cdot\left[\vec{g} + \ddot{\vec{R}}\right] = M_{\nu\mu} g_\nu a_\mu + \ddot{M}_{\nu\lambda} M_{\nu\mu} R_\lambda a_\mu = M_{\nu\mu} g_\nu a_\mu + T_{\lambda\mu} R_\lambda a_\mu \ . \qquad \text{(A-3)}$$

Because it is tedious to calculate the complete exact expression for matrix $\boldsymbol{T}$, we used the symbolic manipulation program MAPLE to do the algebra. The expressions are listed below.

$$\begin{aligned}
T_{11} &= -\dot{\phi}^2 \cos^2\rho - \dot{\rho}^2 \\
T_{12} &= -\ddot{\phi}\cos\rho\cos\psi + \ddot{\rho}\sin\psi + 2\dot{\phi}\dot{\rho}\sin\rho\cos\psi + \dot{\phi}^2\cos\rho\sin\rho\sin\psi \\
T_{13} &= -\ddot{\rho}\cos\psi - \ddot{\phi}\cos\rho\sin\psi + 2\dot{\phi}\dot{\rho}\sin\rho\sin\psi - \dot{\phi}^2\cos\rho\sin\rho\cos\psi \\
T_{21} &= \ddot{\phi}\cos\rho\cos\psi - 2\dot{\rho}\dot{\psi}\cos\psi - \ddot{\rho}\sin\psi - 2\dot{\phi}\dot{\psi}\cos\rho\sin\psi + \dot{\phi}^2\cos\rho\sin\rho\sin\psi \\
T_{22} &= -\dot{\psi}^2 - \dot{\rho}^2\sin^2\psi - \dot{\phi}^2\left(1-\cos^2\rho\sin^2\psi\right) + 2\dot{\phi}\dot{\psi}\sin\rho + 2\dot{\phi}\dot{\rho}\cos\rho\cos\psi\sin\psi \qquad \text{(A-4)} \\
T_{23} &= -\ddot{\psi} + \ddot{\phi}\sin\rho + 2\dot{\phi}\dot{\rho}\sin^2\psi + \left(\dot{\rho}^2 - \dot{\phi}^2\cos^2\rho\right)\cos\psi\sin\psi \\
T_{31} &= \ddot{\rho}\cos\psi + \ddot{\phi}\cos\rho\sin\psi + 2\dot{\phi}\dot{\psi}\cos\rho\cos\psi - 2\dot{\rho}\dot{\psi}\sin\psi - \dot{\phi}^2\cos\rho\sin\rho\cos\psi \\
T_{32} &= \ddot{\psi} - \ddot{\phi}\sin\rho - 2\dot{\phi}\dot{\rho}\cos\rho\cos\psi + \left(\dot{\rho}^2 - \dot{\phi}^2\cos^2\rho\right)\cos\psi\sin\psi \\
T_{33} &= -\dot{\psi}^2 - \dot{\rho}^2\cos^2\psi - \dot{\phi}^2\left(1-\cos^2\rho\cos^2\psi\right) + 2\dot{\phi}\dot{\psi}\sin\rho - 2\dot{\phi}\dot{\rho}\cos\rho\cos\psi\sin\psi
\end{aligned}$$

These exact expressions are included only for completeness. In the analysis of the towbody motion, only T_{32} was used to determine towbody orientation. When the roll and pitch angles are small, as was the case here, it is necessary to retain only terms of first order in ρ, ψ and $\dot{\phi}$.

In the flight tests reported here and in Ref.[1], the forward accelerometer (A_L) was mounted on

the axis of the cylinder 0.33 m above the suspension point (i.e. $\vec{R} = R\hat{e}_3$; $R = 0.33\text{m}$). Thus the forward accelerometer signal is, from (A-3) and (A-4) and after calibrating the signal,

$$\begin{aligned} A_L(t) &= gM_{32}(t) + RT_{32}(t) \\ &\sim R\ddot{\psi} - g\psi \qquad . \end{aligned} \tag{A-5}$$

Comparison of the forward magnetometer and the forward accelerometer at frequencies where the towbody motion is basically a pure pitching motion shows that (A-5) is essentially exact. A similar equation cannot be written for the roll motion because the bridle restrains the towbody so that the centre of rolling motion is not well defined. Therefore we did not use the transverse accelerometer in estimating the towbody motions listed in Tables II and III.

(v) Magnetometer Signals

The output of a vector magnetometer is the projection of the Earth's magnetic field on the gain vector. The algebra is similar to that for the accelerometers. The magnetometer gain is denoted by

$$\vec{b} = b_\mu \hat{e}_\mu \quad \text{(Body fixed)},$$

and the Earth's magnetic field is

$$\vec{B}_0 = B_0(\hat{u}_2 \sin\beta - \hat{u}_3 \cos\beta) \quad \text{(Space fixed)}.$$

β is the angle between the magnetic field and 'down' ($-\hat{u}_3$). Thus the magnetometer output is

$$B(t) = \vec{b}(t)\cdot\vec{B}_0 = M_{\mu\nu}B_{0\mu}b_\nu = B_0\left[M_{2\nu}b_\nu \sin\beta - M_{3\nu}b_\nu \cos\beta\right] \quad . \tag{A-6}$$

In the flight trial described here, the magnetometers were very nearly aligned with the towbody axes so the complete expressions for the magnetometer outputs after offsets are removed and the gain is included are

$$\begin{aligned} B_T &= B_1 = B_0\left[-\sin\beta\sin\phi\cos\rho + \cos\beta\sin\rho\right] \quad , \\ B_L &= B_2 = B_0\left[\sin\beta\cos\phi\cos\psi + \cos\beta\cos\rho\sin\psi + \sin\beta\sin\phi\sin\rho\sin\psi\right] \quad , \\ B_V &= B_3 = B_0\left[\sin\beta\cos\phi\sin\psi - \cos\beta\cos\rho\cos\psi - \sin\beta\sin\phi\sin\rho\cos\psi\right] \quad . \end{aligned} \tag{A-7}$$

The expressions in (A-7) can be simplified by making small-angle approximations where the yaw and pitch are expressed as small deviations (α, τ, γ) from the average values (ϕ_0, ρ_0, ψ_0) :

$$\begin{aligned} \text{Yaw} &: \ \phi = \phi_0 + \alpha \, , \\ \text{Roll} &: \ \rho = \rho_0 + \tau \\ \text{Pitch} &: \ \psi = \psi_0 + \gamma . \end{aligned}$$

In previous analyses, it was assumed that the time-averaged roll was small. However, the flight test of 21 March 1997 showed roll angles up to 3°. In the flight trial in Oct. 1996, the static pitch angle ψ_0 was always <5°, and in March 1997 it was <3°. The small angle expressions for the magnetometer outputs become

$$\frac{B_T}{B_0} = -\sin\beta\sin\phi_0 + \rho_0\cos\beta \;-\; \alpha\sin\beta\cos\phi_0 + \tau(\cos\beta + \rho_0\sin\beta\sin\phi_0) \;,$$

$$\frac{B_L}{B_0} = \sin\beta\cos\phi_0 + \psi_0\cos\beta + \rho_0\psi_0\sin\beta\sin\phi_0 \;-\; \alpha\sin\beta\sin\phi_0 + \tau\psi_0\sin\beta\sin\phi_0 + \gamma(\cos\beta - \psi_0\sin\beta\cos\phi_0 + \rho_0\sin\beta\sin\phi_0) \;, \tag{A-8}$$

$$\frac{B_V}{B_0} = -\cos\beta + \psi_0\sin\beta\cos\phi_0 - \rho_0\sin\beta\sin\phi_0 \;-\; \alpha\psi_0\sin\beta\sin\phi_0 + \tau(-\sin\beta\sin\phi_0 + \rho_0\cos\beta) + \gamma(\sin\beta\cos\phi_0 + \psi_0\cos\beta) \;.$$

In order to use the same notation for the forward accelerometer, A_L at frequency f is expressed as

$$\frac{A_L}{g} = -\psi_0 - \gamma\left(1 + \frac{4\pi^2 f^2 R}{g}\right) \;. \tag{A-8a}$$

(vi) Power-Spectral Analysis

The linearized expressions for the sensor outputs given in eqs. (A-8) and (A-8a) can be written compactly as

$$S_j = C_j + A_j\alpha + R_j\tau + Q_j\gamma \tag{A-9a}$$

where

$$S_1 = \frac{B_T}{B_0} \;;\; S_2 = \frac{B_L}{B_0} \;;\; S_3 = \frac{B_V}{B_0} \;;\; S_4 = \frac{A_L}{g} \;. \tag{A-9b}$$

Using the notation of (A-9a), P_{ij} the cross power of signals S_i and S_j can be given in terms of the cross powers of the rotation angles α,τ and γ

$$\mathrm{Re}(P_{ij}) = A_iA_jP_{\phi\phi} + (A_iR_j + A_jR_i)\mathrm{Re}(P_{\phi\tau}) + (A_iQ_j + A_jQ_i)\mathrm{Re}(P_{\phi\psi}) + R_iR_jP_{\tau\tau} + (R_iQ_j + R_jQ_i)\mathrm{Re}(P_{\tau\psi}) + Q_iQ_jP_{\psi\psi} \quad ; \qquad \text{(A-10a)}$$

$$\mathrm{Im}(P_{ij}) = (A_iR_j - A_jR_i)\mathrm{Im}(P_{\phi\tau}) + (A_iQ_j - A_jQ_i)\mathrm{Im}(P_{\phi\psi}) + (R_iQ_j - R_jQ_i)\mathrm{Im}(P_{\tau\psi}) \quad . \text{(A-10b)}$$

Determining the towbody motion in a frequency band by cross-power spectral analysis consists of the following procedure :

1. Calculate the complex Discrete Fourier Transforms F_j of signals S_j, j=1,...,4. The DFTs are normalized so $|F_j|^2$ is the power spectrum normalized to Hz^{-1}.

2. Calculate the cross powers by summing over the specified frequency band :

$$P_{ij} = \left(\sum F_iF_j^*\right)df$$

where df is the frequency per point. The physical dimension of P_{ij} is the product of the dimensions of S_i and S_j.

3. Calculate the cross powers of the rotation angles, $P_{\phi\phi}$, $P_{\phi\rho}$, $P_{\phi\psi}$, $P_{\tau\tau}$, $P_{\tau\psi}$, $P_{\psi\psi}$ (6 real and 3 imaginary powers) by a least-squares fit to the measured cross powers (10 real and 6 imaginary powers) using (A-10a) and (A-10b). It appears that there are 4 degrees of freedom in the fit to the real cross powers and 3 degrees for the imaginary, but only two of the three magnetometer signals are independent and thus the fits are not really overdetermined. In addition, there are three constraints on the solution :

$$|P_{\phi\tau}| \le \sqrt{P_{\phi\phi}P_{\tau\tau}} \quad ,$$

$$|P_{\phi\psi}| \le \sqrt{P_{\phi\phi}P_{\psi\psi}} \quad , \qquad \text{(A-11)}$$

$$|P_{\tau\psi}| \le \sqrt{P_{\tau\tau}P_{\psi\psi}} \quad .$$

UNCLASSIFIED

SECURITY CLASSIFICATION OF FORM
(highest classification of Title, Abstract, Keywords)

DOCUMENT CONTROL DATA

(Security classification of title, body of abstract and indexing annotation must be entered when the overall document is classified)

1. ORIGINATOR (The name and address of the organization preparing the document. Organizations for whom the document was prepared, e.g. Establishment sponsoring a contractor's report, or tasking agency, are entered in section 8.)

Defence Research Establishment Atlantic/DRED
P.O. Box 1012, Dartmouth, N.S.,Canada B2Y 3Z7

2. SECURITY CLASSIFICATION (Overall security of the document including special warning terms if applicable.)

UNCLASSIFIED

3. TITLE (The complete document title as indicated on the title page. Its classification should be indicated by the appropriate abbreviation (S,C.R or U) in parentheses after the title.)

Second Flight Test of a Towbody for a SQUID Gradiometer

4. AUTHORS (Last name, first name, middle initial. If military, show rank, e.g. Doe, Maj. John E.)

WILSON, Harold S., RELIGA, Richard J. and DUSTAN, Brian W.

5. DATE OF PUBLICATION (Month and year of publication of document.)

June 1997

6a. NO. OF PAGES (Total containing information. Include Annexes, Appendices, etc.)

23

6b. NO. OF REFS. (Total cited in document.)

6

7. DESCRIPTIVE NOTES (The category of the document, e.g. technical report, technical note or memorandum. If appropriate, enter the type of report, e.g. interim, progress, summary, annual or final. Give the inclusive dates when a specific reporting period is covered.)

Technical Memorandum

8. SPONSORING ACTIVITY (The name of the department project office or laboratory sponsoring the reseach and development. include the address.)

CRAD - DSAA

9a. PROJECT OR GRANT NUMBER (If appropriate, the applicable research and development project or grant number under which the document was written. Please specify whether project or grant.)

Project 1.C.D

9b. CONTRACT NUMBER (If appropriate, the applicable number under which the document was written.)

10a. ORIGINATOR'S DOCUMENT NUMBER (The official document number by which the document is identified by the originating activity. This number mrst be unique to this document.)

DREA Technical Memorandum 97/238

10b. OTHER DOCUMENT NUMBERS (Any other numbers which may be assigned this document either by the originator or by the sponsor.)

11. DOCUMENT AVAILABILITY (Any limitations on further dissemination of the document, other than those imposed by security classification)

(X) Unlimited distribution
( ) Distribution limited to defence departments and defence contractors; further distribution only as approved
( ) Distribution limited to defence departments and Canadian defence contractors; further distribution only as approved
( ) Distribution limited to government departments and agencies; futher distribution only as approved
( ) Distribution limited to defence departments; further distribution only as approved
( ) Other (please specify):

12. DOCUMENT ANNOUNCEMENT (Any limitation to the bibliographic annoucement of this document. This will normally correspond to the Document Availability (11). However, where futher distribution (beyond the audience specified in 11) is possible, a wider announcement audience may be selected.)

Unlimited

UNCLASSIFIED

SECURITY CLASSIFICATION OF FORM

DCD03 2/06/87

13. ABSTRACT (a brief and factual summary of the document. It may also appear elsewhere in the body of the document itself. It is highly desirable that the abstract of classified documents be unclassified. Each paragraph of the abstract shall begin with an indication of the security classification of the information in the paragraph (unless the document itself is unclassified) represented as (S), (C), (R), or (U). It is not necessary to include here abstracts in both official languages unless the text is bilingual).

This report presents the results of the second flight test of a towbody for a vertical-dewar superconducting magnetic gradiometer. The towbody was modified by the addition of a weight at the bottom in an attempt to reduce aerodynamic instabilities that were encountered in the first flight. Acceleration power spectra are presented and magnetometer slew rates and yaw, roll, and pitch amplitudes are given as tables. The pitching instability previously observed near 45 knots did not appear in this test and the high speed roll/yaw instability appeared only above 75 knots in level flight. The effect of magnetic contamination of the added weight is discussed and it is concluded that it should not be a problem during the flight test of a gradiometer. An Appendix gives the algebra required in the data analysis.

14. KEYWORDS, DESCRIPTORS or IDENTIFIERS (technically meaningful terms or short phrases that characterize a document and could be helpful in cataloguing the document. They should be selected so that no security classification is required. Identifiers, such as equipment model designation, trade name, military project code name, geographic location may also be included. If possible keywords should be selected from a published thesaurus. e.g. Thesaurus of Engineering and Scientific Terms (TEST) and that thesaurus-identified. If it not possible to select indexing terms which are Unclassified, the classification of each should be indicated as with the title).

Aerodynamics
Towbody
Finite cylinder
Crossflow
High angle of attack

#508793